36F.0 MICROSTRUCTURE AND PROCESSING LINKS IN BETA-TITANIUM DURING ADDITIVE MANUFACTURING

Chris Jasien (Mines)
Faculty: Amy Clarke (Mines)
Industrial Mentor: John Foltz (ATI) and Lee Semiatin (AFRL)

This project initiated in Fall 2020 and is supported by the Office of Naval Research (ONR). The research performed during this project will serve as the basis for a Ph.D. thesis program for Chris Jasien.

36F.1 Project Overview and Industrial Relevance

The continued development of metal additive manufacturing (AM) over the past couple decades has expanded the applications and material classes in which these processes can be used. Titanium alloys have been at the center of this development due to their superior properties, particularly for aerospace and defense applications. Although Ti-6Al-4V has typically dominated in terms of use and research pertaining to metal AM processes, β-titanium alloys have begun to find increased use over Ti-6Al-4V (an α + β alloy), due to their increased strength-to-density ratios, among other properties. These β-titanium alloys differ from other classifications of titanium in that, upon quenching to room temperature from the β phase field, they may transform martensitically, or the metastable β-phase may be retained [36.F2-3].

There has been extensive investigation on the response of Ti-6Al-4V to various AM processing techniques, but there is still much to be understood when it comes to β-titanium. For this reason, this project focuses on investigating solidification and microstructure evolution of selected β-titanium alloys during AM. This includes understanding the columnar to equiaxed transition (CET) for a variety of thermal conditions, as well as thermal history effects on the microstructure. The study of β-titanium alloys will also avoid the confounding solid-state phase transformations that occur in Ti-6Al-4V during solidification. In-situ radiography experiments performed at the Advanced Photon Source (APS) at Argonne National Laboratory of simulated laser-powder bed fusion (L-PBF) of Ti-10V-2Fe-3Al (wt.%) (Ti-1023), a β-titanium alloy, allow for the determination of solid-liquid interface velocities (V) for various solidification conditions. In conjunction with these velocities, finite element analysis (FEA) simulations, using tools such as FLOW-3D®, are also perform. These simulations provide other useful information, including predicted thermal gradients (G), which aid in understanding the effect of AM processing conditions on as-built microstructures. Investigation of other β-titanium alloys for L-PBF and other AM processes is also planned as part of this project.

36F.2 Previous Work

36F.2.1 FLOW-3D Simulations

In order to better capture the intricacies of L-PBF processing, a commercial computational fluid dynamics software, FLOW-3D, was utilized to model simulated Ti-1023 AM experiments performed at the APS. The models were calibrated using maximum width and depth measurements from the in-situ x-ray radiography as well as the observed laser mode (conduction or keyholing). Predicted solidification velocity profiles from these models matched closely with those obtained from the in-situ x-ray radiography. Additionally, the models were able to capture the rapid increase in velocity at the final stages of solidification, something the experiments, which had limited spacial and temporal resolution, were unable to capture. Thermal gradient predictions were also used in conjunction with solidification velocities to investigate the models' ability to predict grain morphologies. For both spot-melts and rasters, the FLOW-3D G-V conditions and predicted as-built microstructure matched those observed from top-down secondary electron imaging (SEI) of the experiments.

36F.3 Recent Progress

36F.3.1 Ti-5Al-5V-5Mo-3Cr Equilibrium Alpha-Transus Determination

To determine the equilibrium alpha transition temperature of Laser Power Bed Fusion (LPBF) produced Ti-5Al-5V-5Mo-3Cr (Ti-5553) (wt.%), controlled heating rate experiments using a TA Instruments 805L Quench Dilatometry

were performed on samples extracted from the middle of a nominal parameter build provided by Kansas City National Security Campus (KCNSC). Dilatometry experiments allow for the measurement of change in length of a sample as a function of temperature, where significant deviations from linear thermal expansion behavior indicate a phase transformation. For this work, the transformation of importance was the metastable BCC β phase to equilibrium HCP α phase. The temperature at which this transformation occurs is typically referred to as the alpha-transition (transus) temperature. To determine this temperature for Ti-5553, four different heating rates, listed below in **Table 1**, were performed. The initial and final conditions of a typical heating profile are shown in **Figure 1**. Upon completion of all the dilatometry trials, there was a noticeable effect of heating rate on phase formation and the temperature regimes over which they occurred. Representative responses for each of the heating rates is presented below in **Figure 2**. The fastest heating rate (10°C/s) shows only one noticeable slope change. However, for the slower heating rates, additional changes are observed, suggesting more phases are allowed to form as the heating rate is decreased. Additionally, the temperature regimes of these transformations shift to lower temperatures as the heating rate is decreased. In order to better understand these phase changes, it was necessary to know the starting microstructure of the dilatometry samples. As-quenched metastable β-Ti alloys such as Ti-5553 have been reported to consist of the β-phase and uniformly distributed athermal ω (ω_a) using transmission electron microscopy (TEM) [36F.4-5]. However, in as-built LPBF specimens, X-ray diffraction (XRD) has only shown the existence of the β-phase [36.F6-7]. This discrepancy is most likely a result of the achieved resolution of TEM compared to XRD. For this reason, it was likely that the initial dilatometry samples used in this study consisted of both β and ω_a.

The observed phase transformations in **Figure 2** are labeled below in **Figure 3** for a 0.1°C/s and 10°C/s sample. As the samples were heated up to point A, the length increased as a result of thermal expansion. At point A, the sample started to contract as hexagonal isothermal ω (ω_{iso}) began to form until point B where the transformation stopped. This phase formed regardless of the heating rate, which is contrary to what has been previously reported in literature. Using high energy XRD (HEXRD), ω_{iso} formation was unobservable above heating rates of 0.1°C/s according to Settefrati et al. [36F.4]. Further heating returned the sample to a region of pure thermal expansion. When the temperature is further raised, a sharp length increase is seen at point C in **Figure 3a**. This marks the start of alpha transformation from the ω_{iso}. However, no such sharp increase is observed in **Figure 3b**. This difference suggests the formation of an intermediate phase before HCP α that occurs only at slow heating rates. This phase is orthorhombic α'', which only forms at heating rates below 3°C/s [36F.4] and also explains the lack of noticeable slope change in the high heating rate sample (**Figure 3b**). The direct transformation of ω_{iso} to α does not result in an obvious volume change because these phases both have hexagonal crystal structures. A slight deviation in linearity at point E may suggest the beginning of the α transformation. Point C in **Figure 3a** corresponds to the transformation of hexagonal to orthorhombic (ω_{iso} to α'') and point D the orthorhombic back to hexagonal (α'' to α). To further investigate the effect of heating rate, starting and ending ω_{iso} formation temperatures as well as transformed volume fractions of ω_{iso} were determined for each sample using a lever rule approach [36F.8]. It is important to understand the formation of ω_{iso} in metastable β-Ti alloys because this phase has been suggested to provide preferential nucleation sites for α formation [36F.9]. From **Figure 4**, as the heating rate is increased, the temperature regime over which ω_{iso} formation occurs, also increases. This shows that heating rate heavily influences the kinetics of this transformation. The presence of ω_{iso} at lower temperatures results in the formation of α at lower temperatures, as illustrated in **Figure 2**. It is less clearly seen in the 10°C/s condition in **Figure 2** due to the possibility of a different α formation mechanism taking place. Duerig et al. suggested at high aging temperatures, preferential nucleation of α off of ω_{iso} no longer occurs [36F.1]. Instead, small amounts of α precipitates randomly form within the interior of the grains that results in a reduced driving force for α formation as the β-transus is approached. Although the 10°C/s dilatometry samples were not aged, this high temperature mechanism is likely occurring for there is insufficient time for α nucleation off the preexisting ω_{iso} due to the fast heating rate. The final aspect of this work was the extraction of the alpha-transus from each dilatometry experiment. It was difficult to determine a repeatable method which to apply due to the differing evolution of phases for each heating rate. For this reason, two techniques were utilized to estimate the alpha-transus, one for the highest heating rate and another for the other heating rates. **Figure 5** shows an example of how each method was applied to the dilatometry data. In **Figure 5a**, a regression line was determined before and after the approximate alpha transformation. These lines were then interpolated and the temperature at which they intersected was taken as the estimated alpha-transus. To obtain the estimated α'' transformation temperature, the same approach was utilized taking the regions before and after the α'' region. The lack of an observable alpha transformation region for the 10°C/s samples required a different method. A regression line was calculated from the region after complete ω_{iso} transformation and before any predicted alpha formation (~450-600°C). The difference between the experimental

data and regression line was then determined and plotted as a function of temperature (**Figure 5b**). A local maximum appeared, and the corresponding temperature was taken as the estimated alpha-transus. This maximum deviation from linearity was assumed to be the region where alpha transformation occurred. An α'' transformation was not determined for this heating rate because one does not occur, as discussed previously.
Using these methods, extraction was completed for each sample and the average estimated α'' and alpha-transus for each heating rate are listed and plotted below in **Table 2** and **Figure 6** respectively. From **Figure 6**, as the heating rate is decreased, the α'' transition temperature also decreases and appears to begin 'leveling-off'. Suggesting that equilibrium is being approached. However, the alpha-transus, shown in **Figure 6b**, does not exhibit this trend at the slowest heating rate. It is not immediately clear why this discrepancy exists. For when the α'' transformation occurs at lower temperatures, alpha transformation should occur at lower temperatures as well. It is possible that additional transformations occur during the slowest heating rate, which complicate the extraction of an accurate alpha-transus. No literature has been reported on heating rates in the range of 0.01°C/s so it is unclear what causes the perceived increase in alpha-transus.

36F.4 Plans for Next Reporting Period

- Cross-section microstructural characterization of Ti-1023 spot-melt and raster APS samples
- Fabrication and microstructural characterization of varying AM process conditions using other Beta-Ti alloys

36F.5 References

[36F.1] T. W. Duerig, G. T. Terlinde, and J. C. Williams, "Phase transformations and tensile properties of Ti-10V-2Fe-3AI," *Metall. Trans. A*, vol. 11, no. 12, pp. 1987–1998, Dec. 1980, doi: 10.1007/BF02655118.

[36F.2] T. W. Duerig and J. C. Williams, "Beta Titanium Alloys in the 80s: Proceedings of the Symposium," *Metall. Soc. AIME*, pp. 19–67, 1984.

[36F.3] G. Lütjering and J. C. Williams, Eds., "Fundamental Aspects," in *Titanium*, Berlin, Heidelberg: Springer, 2007, pp. 15–52. doi: 10.1007/978-3-540-73036-1_2.

[36F.4] A. Settefrati *et al.*, "Precipitation sequences in beta metastable phase of Ti-5553 alloy during ageing," p. 4.

[36F.5] J. Coakley *et al.*, "Precipitation processes in the Beta-Titanium alloy Ti–5Al–5Mo–5V–3Cr," *J. Alloys Compd.*, vol. 646, pp. 946–953, Oct. 2015, doi: 10.1016/j.jallcom.2015.05.251.

[36F.6] H. Schwab, M. Bönisch, L. Giebeler, T. Gustmann, J. Eckert, and U. Kühn, "Processing of Ti-5553 with improved mechanical properties via an in-situ heat treatment combining selective laser melting and substrate plate heating," *Mater. Des.*, vol. 130, pp. 83–89, Sep. 2017, doi: 10.1016/j.matdes.2017.05.010.

[36F.7] H. Schwab, F. Palm, U. Kühn, and J. Eckert, "Microstructure and mechanical properties of the near-beta titanium alloy Ti-5553 processed by selective laser melting," *Mater. Des.*, vol. 105, pp. 75–80, Sep. 2016, doi: 10.1016/j.matdes.2016.04.103.

[36F.8] Q. Hui, X. Xue, H. Kou, M. Lai, B. Tang, and J. Li, "Kinetics of the ω phase transformation of Ti-7333 titanium alloy during continuous heating," *J. Mater. Sci.*, vol. 48, no. 5, pp. 1966–1972, Mar. 2013, doi: 10.1007/s10853-012-6962-5.

[36F.9] M. Blackburn and J. C. Williams, "Phase transformations in titanium-molybdenum and titanium-vanadium alloys," *Trans. Metall. Soc. AIME*, vol. 242, p. 2461, 1968.

36F.6 Figures and Tables

Table 1: Nominal heating rates and number of desired samples to be tested for each rate.

Number of Samples	Heating Rate (°C/s)
6	10
7	1
7	0.1
7	0.01

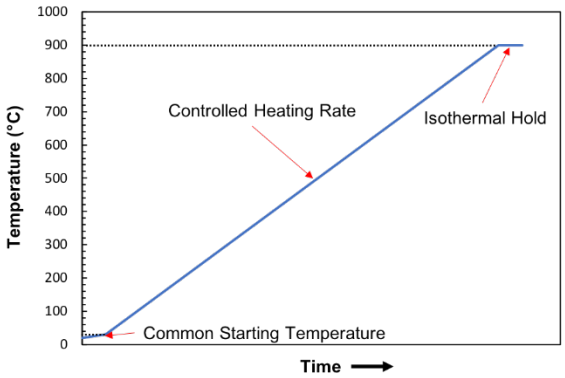

Figure 1: Typical elements of the temperature profiles used during the dilatometer experiments.

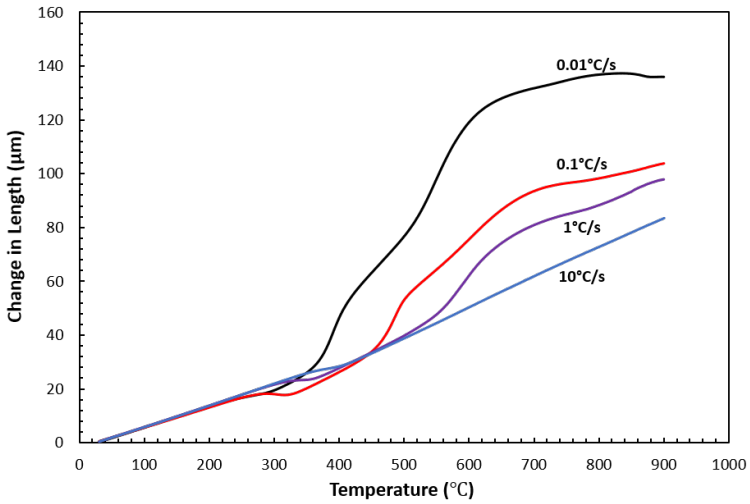

Figure 2: Representative change in length as a function of temperature curves for heating rates of 10°C/s, 1°C/s, 0.1°C/s, and 0.01°C/s.

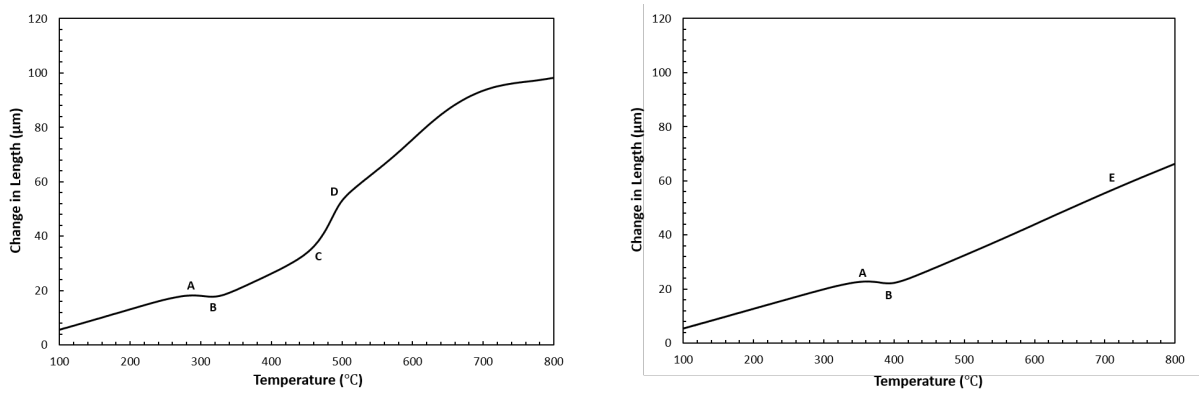

(a) **(b)**

Figure 3: Dilatometry curves with labeled points showing locations of interest for heating rates of **(a)** 0.1°C/s and **(b)** 10°C/s.

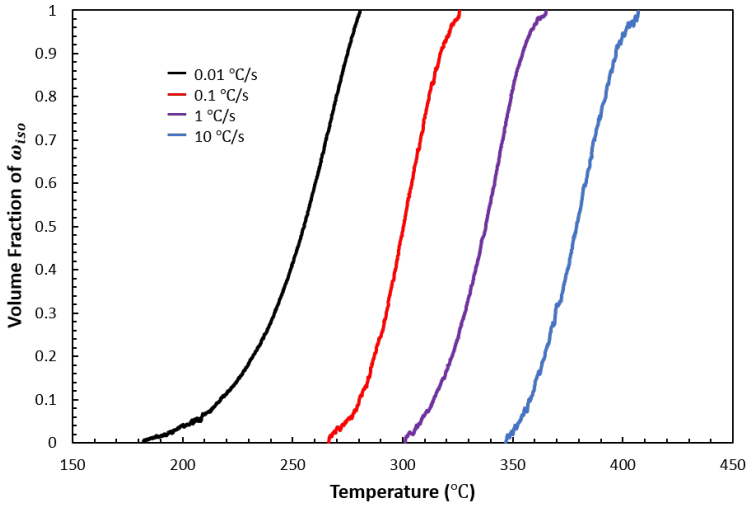

Figure 4: Formation of ω_{iso} as a function of temperature for the four investigated heating rates.

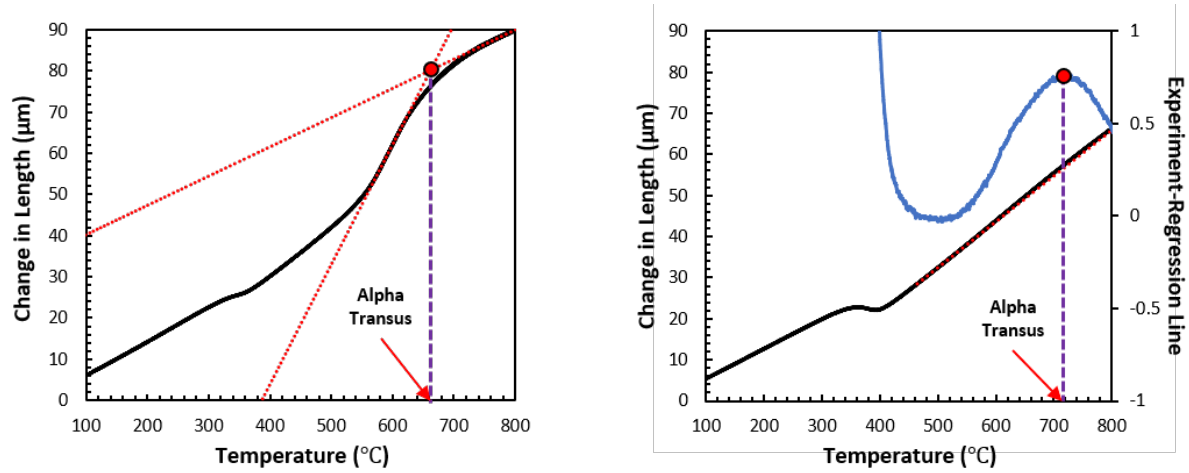

(a) **(b)**

Figure 5: Schematic of approach used to estimate alpha-transus for **(a)** 0.01, 0.1, and 1°C/s and **(b)** 10°C/s heating rates.

Table 2: Average estimated α'' and alpha-transus temperatures with 95% confidence interval for each heating rate.

Heating Rate (°C/s)	α'' Transus (°C)	Alpha Transus (°C)
10	-	726.16±13.84
1	493.52±6.34	656.47±11.59
0.1	424.06±4.12	496.22±5.67
0.01	399.66±4.13	516.52±6.75

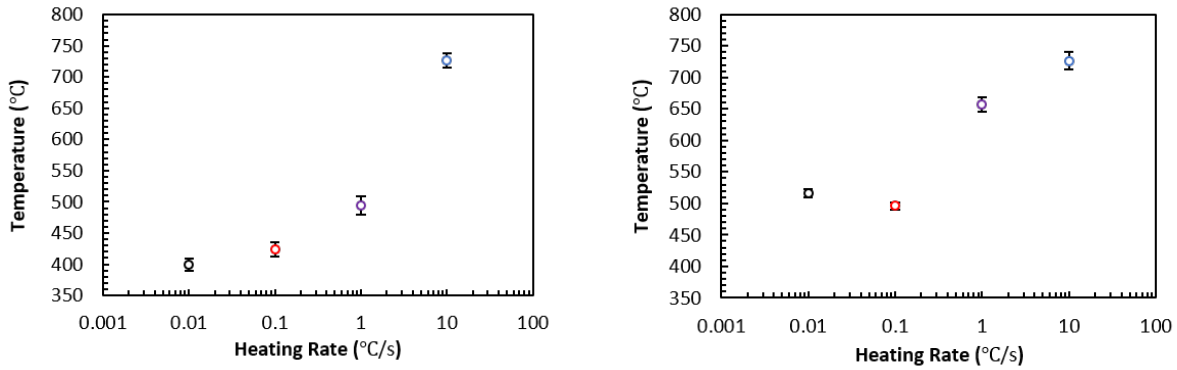

(a) **(b)**

Figure 6: Semi-log plot of **(a)** α'' transus and **(b)** alpha-transus as a function of heating rate. Note: the error bars are upper and lower 95% confidence intervals and the transformation temperature for the 10°C/s condition in **(a)** corresponds to the alpha-transus.